

DELINEATING FLOOD EXTENT AND FLOOD-PRONE RICE AREAS IN THE PHILIPPINES USING SYNTHETIC APERTURE RADAR

Alice Laborte (1), Jeny Raviz(1), Sonia Asilo (2), Mary Rose Mabalay(2),
Neale Paguirigan(1), Juanito Maloom(2), Mabel Barroga(2), Jesiree Elena Ann Bibar(2), Meriam Coñado(2),
Eve Daphne Radam(2), Jovino de Dios(2), Eduardo Jimmy Quilang(2)

¹International Rice Research Institute (IRRI), Los Baños, Laguna, Philippines

²Philippine Rice Research Institute (PhilRice), Science City of Muñoz, Nueva Ecija, Philippines

Email: a.g.laborte@irri.org; j.raviz@irri.org; slasilo@gmail.com; mro.mabalay@philrice.gov.ph;
n.paguirigan@irri.org; jm.maloom@philrice.gov.ph; mibarroga@gmail.com, jesiree.delatorre@gmail.com;
mv.conado@gmail.com; edo.radam@philrice.gov.ph; jl.dedios@philrice.gov.ph; ejp.quilang@philrice.gov.ph

KEY WORDS: flood assessment, rice production, SAR, typhoon

ABSTRACT: Accurate, timely, and location-specific estimates of damages resulting from natural calamities such as typhoons and floods due to torrential rains are necessary for rapid decision making on emergency response, early assessment of potential shortfalls in food production, and planning and implementation of rehabilitation programs. To deliver timely and actionable information on the impact of typhoon or flood events on rice production in the Philippines, protocols for flood assessment using Synthetic Aperture Radar (SAR) and field surveys have been developed and implemented as part of the Philippine Rice Information System (PRISM, <https://prism.philrice.gov.ph/>), an operational rice monitoring system in the country. This paper presents the flood assessment protocol of PRISM and analysis to identify flood-prone rice areas.

Initially, COSMO SkyMed and TerraSAR-X, both commercially available SAR imagery, were used for rice mapping and flood detection. Starting 2015, Sentinel-1 became the primary source of SAR images for rice mapping and flood assessment in PRISM. A rule-based method is used to classify rice areas every season and a simple change detection and thresholding algorithm is used to map flooded areas. From 2014 to 2018, 25 flood assessments were conducted and these were provided to the National and the Regional Field Offices of the Philippine Department of Agriculture. During the assessment period, the flood events with the most rice areas affected occurred in September and October which coincide with the ripening and peak of harvest for the wet season rice cropping. The most damaging flood event during the assessment period was Typhoon Haima (local name: Lawin) which affected the country in October 2016 and flooded 97 thousand ha, more than half of which were planted to rice. In 2018, Typhoon Mangkhut (local name: Ompong), which made landfall in September, caused flooding in more than 82 thousand ha, more than one-third of which were planted to rice. Results from the multi-year assessments show that nearly 0.3 million ha of rice were flooded in at least two out of five years; and 16 thousand ha were flooded in at least four out of five years. Central Luzon, the top rice-producing region in the country, is by far the most flood-prone region with 116 thousand ha of its rice land flooded in at least two out of five years. Some implications and recommendations to improve the current flood assessment procedure as part of an operational system for monitoring are discussed.

1. INTRODUCTION

Accurate, timely, and location-specific estimates of damage resulting from natural calamities, such as typhoons, floods due to torrential rains, and drought, are necessary for rapid decision making on emergency response, early assessment of potential shortfalls in food production, and planning and implementation of rehabilitation programs. The Philippines is a natural disaster hotspot. The country experiences 20 typhoons annually on average, some of which cause major damage to infrastructure and livelihood. One of the strongest tropical cyclones ever recorded, Typhoon Haiyan (local name: Yolanda), caused massive destruction in the Visayas Islands in November 2013, with an estimated total damage of Php 95.5 billion (NDRRMC, 2014) and rice production losses of 260,000 tons (Blanc and Strobl, 2016). Excessive rainfall, especially during typhoons, can result in continuous inundation and a decrease in plant photosynthesis and respiration (Masutomi et al., 2012). Likewise, strong winds can cause lodging, stripping, and injury of plant organs, and induced water stress due to enforced transpiration (Masutomi et al., 2012). The extent and severity of the damage to rice crops depend on the timing of the typhoon relative to the growth stage of the crop (Blanc and Strobl, 2016).

Extreme weather conditions are very likely to be more frequent and intense in the future (IPCC, 2014). In the event of a calamity, immediate on-the-ground assessment is often a challenge because of mobility problems as a result of flood, road obstructions, and infrastructure damage. Remote sensing can play a role in rapid and cost-effective

assessment of damage over a wide area.

Remotely sensed data, specifically satellite imagery, have been used to map flood in various regions. Synthetic Aperture Radar (SAR) is particularly useful for mapping flood because it can provide frequent observations in almost any weather condition. Cian et al. (2018) reviewed flood mapping studies using SAR that were conducted between 2000 and 2017. These studies used different sensors (ERS-1, ENVISAT ASAR, TerraSAR-X, COSMO SkyMed, Radarsat, and Sentinel-1) and methodological approaches including unsupervised classification, active contour models, thresholding, and probabilistic change detection.

The Philippine Rice Information System (PRISM), a collaborative project funded by the Philippine Department of Agriculture (DA) through the Bureau of Agricultural Research, developed and implemented protocols for monitoring rice areas and assessment of damage to the rice crop due to flood or drought using remote sensing and field surveys. This paper describes the methods used by PRISM and presents analyses of results of flood assessments conducted from 2014 to 2018. Finally, some recommendations to improve the current flood assessment procedure are discussed.

2. MATERIALS AND METHODS

2.1 Data

Satellite imagery: SAR is an active sensor that can penetrate clouds and can be used day or night, even during the monsoon season, making it ideal for flood assessments. Initially, COSMO SkyMed (CSK) and TerraSAR-X (TSX), both commercially available SAR imagery, were used in flood assessments (Table 1). A year after its launch, Sentinel-1 A/B (S1) became the primary source of SAR data for flood assessments. In cases when available S1 data over an affected area did not coincide with dates of flooding, TSX data were acquired. For each location, at least two images from the same sensor with the same polarization and observation geometry were used. One was a pre-flood image and at least one image was acquired during the flood event.

Table 1. Satellite data used in the flood assessments and their characteristics.

Characteristic	Sentinel-1A/B (S1)	TerraSAR-X (TSX)	COSMO SkyMed (CSK)
Sensor	Active (radar)	Active (radar)	Active (radar)
Product (mode)	Interferometric Wide Swath	ScanSAR	Stripmap
Band(s)/wavelength	C band (5.5 cm)	X band (3.1 cm)	X band (3.1 cm)
Polarization	VV	HH	HH
Spatial resolution (m)	20	18.5	3
Swath width (km)	250 × 250	100 × 150	40 × 40
Repeat cycle (days)	6/12	11	16 (per satellite, 4 satellites)
Image availability	Free	Commercial	Commercial
Year of launch	2014 (S1A), 2016 (S1B)	2007	2007 (CSK-1,2), 2008 (CSK-3), 2010 (CSK-4)
Source	European Space Agency (ESA)	Airbus Defence and Space	Italian Space Agency

Rice map: Preliminary rice area, start of season (SoS), and peak of SAR (PoS) maps generated at the time of flood assessment from 2014 to 2018 using the method described in Nelson et al. (2014) were used to delineate rice areas at risk and affected by typhoon/flood. Following the same procedure, end of season rice maps had accuracy levels ranging from 85% to 93% from 2015 wet season to 2018/19 dry season.

Typhoon advisories and flood reports: Typhoon advisories from the Philippine Atmospheric Geophysical and Astronomical Services Administration (PAGASA) were used as the basis for identifying areas to be assessed (PAGASA, 2019). The forecasted typhoon track, landfall, and intensities were used to identify dates and scenes of

SAR images to be downloaded (for S1) or ordered (TSX, CSK). In case of flood assessment caused by heavy rains, the basis for identifying areas was reports received from the DA Regional Field Offices (RFOs).

Other data: The 90-m Digital Elevation Model (DEM) from the Shuttle Radar Topography Mission (SRTM) was used in the flood assessment for masking out high-elevation and sloping areas. The latter removes potential misclassification of shadows as flooded areas in SAR images.

To estimate rice area by administrative level (region, province, municipality), the administrative map from the Philippine Statistics Authority (PSA) was used.

2.2 The PRISM flood assessment protocol

Upon receipt of a request from the DA national and/or regional offices and based on weather advisory from PAGASA, PRISM performs flood assessment following a protocol (Figure 1) that includes the identification of the area to be assessed and SAR images to acquire, processing of SAR data, and rapid field appraisal.

In case a typhoon is headed to the Philippines, weather advisories on the typhoon's forecasted intensity and track from PAGASA were monitored closely to identify the areas likely to be affected and the track(s), scene(s), and dates of the SAR images to be acquired. In the current protocol, an initial assessment providing estimates of area with standing rice crops that will most likely be affected by the typhoon/flood based on the PAGASA weather advisory is submitted within three days after the request from the DA. Within 10 days, a more detailed assessment that includes estimates of rice areas affected by typhoon/flood is submitted. The delivery of the complete assessment depends on the availability of satellite images and the rapid field appraisal.

Rice areas at risk: These are rice areas that are most likely not yet harvested (i.e., vegetative to ripening) at the time of the flood event. This initial assessment was included in the PRISM protocol starting in 2016 at the request of the DA for rapid initial estimates to guide them in resource mobilization and prepare for early response.

We use the most recent rice map available for the season, including the SoS and PoS maps (for X-band only), that covers the geographic areas at risk based on the PAGASA weather advisory. The PoS refers to maximum tillering for X band (e.g., TSX, CSK).

To estimate rice areas at risk, the crop growth phase at the time of the extreme weather event was identified based on the number of days from PoS (for X band) or SoS (for C band) to the flood event. For X band, we used the following criteria to classify the growth phase: (1) harvested, if the number of days from PoS to the event ≥ 70 days; (2) ripening, if 40–69 days; (3) reproductive, if 5–39 days; and (4) vegetative, if <5 days. For example, if the PoS is 9 August and the flood event is 20 October, there are 72 days from PoS to the flood event; therefore, the rice area will be classified as "harvested." For C-band, we used the following: (1) harvested, if the number of days from SoS to the event is at least 120 days; (2) ripening, if 90–119 days; (3) reproductive, if 55–89 days; and (4) vegetative, if <55 days.

Flood detection: For each area, at least two SAR images from the same sensor with the same polarization and observation geometry were acquired: one reference image (not flooded, acquired before the flood event) and at least one image at the time of the flood event. Twenty-six flood events occurred from 2014 to 2018 for which PRISM conducted 25 flood assessments (Table 2). Two typhoons occurred immediately after the other, hence only one assessment was conducted.

The original SAR data were processed to obtain terrain geo-coded backscatter following the same procedure as in the basic processing of images for rice mapping described in Nelson et al. (2014). The basic processing and the mapping of flooded areas were done using the MAPscape-RICE[®] software.

A simple change detection and thresholding algorithm was followed. Flood was detected if all the following conditions were satisfied:

1. The ratio between the reference SAR image and any of the SAR images acquired during the flood event is greater than the minimum ratio threshold (set to 2, in linear units).
2. The backscatter in any of the SAR image acquired during the flood event is lower than the water threshold (set to 0.045 for HH and 0.05 in VV, in linear units).
3. The elevation is lower than the threshold (set to 700 m).
4. The slope is lower than the threshold (set to 5 degrees).

Table 2. Flood events assessed and SAR images used, 2014-18.

Year and typhoon name / flood event ^a	Date(s) of event	SAR data used	Dates of SAR data used ^b
2014			
Typhoon Rammasun (Glenda)	Jul 13–17	CSK TSX	(Jun 15, Jul 17) (Jul 5, Jul 16), (Jul 7, Jul 18), (Jul 12, Jul 23)
Tropical storm Fung-wong (Mario)	Sep 17–22	TSX	(Sep 10, Sep 21)
Typhoon Hagupit (Ruby)	Dec 4–10	TSX	(Nov 23, 2011, Dec 9)
2015			
Typhoon Mujigae (Kabayan)	Sep 30–Oct 5	S1A	(Sep 20, Oct 2)
Typhoon Koppu (Lando)	Oct 18–19	TSX S1A	(Sep 14, Oct 22) (Sep 28, Oct 22)
Typhoon Melor (Nona)	Dec 12–18	S1A TSX	(Sep 10, Dec 15) (Sep 8, Dec 15), (Jun 23, Dec 16)
2016			
Southwest monsoon (<i>Habagat</i>)	Aug 8–17	S1A TSX	(Apr 23, Aug 21) (May 29, Aug 14), (Jun 9, Aug 14)
Typhoon Sarika (Karen)	Oct 13–16	S1A	(Sep 9, Oct 15)
Typhoon Haima (Lawin)	Oct 17–19	S1A	(Feb 11, Oct 20)
Severe tropical storm Tokage (Marce)	Nov 23–29	S1A	(Apr 23, Nov 25)
Typhoon Nock-ten (Nina)	Dec 23–26	S1B TSX	(Dec 4, Dec 28) (Apr 6, Dec 26)
2017			
Tropical depression (TD) 01W (Auring)	Jan 7–8	S1A	(Nov 22, 2016, Jan 9)
Tail end of cold front	Jan 20	S1A S1B	(Nov 22, 2016; Jan 21) (Dec 4, 2016; Jan 21)
Heavy rains	April to May	S1A	(Mar 3, May 26)
Severe tropical storm Pakhar (Jolina)	Aug 24–26	S1A	(Nov 1, 2016; Aug 28)
Typhoon Doksuri (Maring)	Sep 11–13	S1A	(May 26, Sep 11)
Tropical storm Kai-tak (Urduja)	Dec 17–23	S1A S1B	(Oct 17, Dec 16) (Oct 6, Dec 17), (Oct 19, Dec 18)
Typhoon Tembin (Vinta)	Dec 20–22	S1A S1B	(Sep 16, Dec 21), (Oct 24, Dec 23) (Oct 24, Dec 23)
2018			
Tropical storm Son-Tinh (Henry)	Jul 16-17	S1B	(Jul 8, Jul 20)
Severe tropical Storm Ampil (Inday)	Jul 17-21	S1B	(Jul 8, Jul 20)
Tropical depression 13W (Josie)	Jul 21-22	S1A	(Jul 15, Jul 27)
Tropical storm Yagi (Karding)	Aug 7-11	S1B	(Aug 1, Aug 13)
Tropical depression 24W (Luis)	Aug 23-24	S1B	(Oct 17, 2017, Aug 25)
Typhoon Mangkhut (Ompong)	Sep 12-15	S1A	(Oct 15, 2017, Sep 16)
Typhoon Yutu (Rosita)	Oct 27-31	S1A	(Oct 3, 2017, Nov 3)
Tropical depression 35W (Usman)	Dec 25-31	S1B	(Dec 18, Dec 30)

^aLocal names are enclosed in parentheses. ^bEnclosed in parentheses are the SAR image pairs. Date before the comma is the acquisition date of the reference image and the date after refer to the image acquired during the flood event. Pairs of dates in the same row but in different parentheses refer to different satellite tracks. Unless otherwise indicated, the dates refer to the same year.

The flood map was overlaid with the rice map and areas were calculated for total flooded and flooded rice using the administrative map. The flood map was also overlaid with the rice map by growth phase to calculate flooded rice areas by growth phase. Estimates of areas at the regional and provincial levels were calculated using ArcGIS.

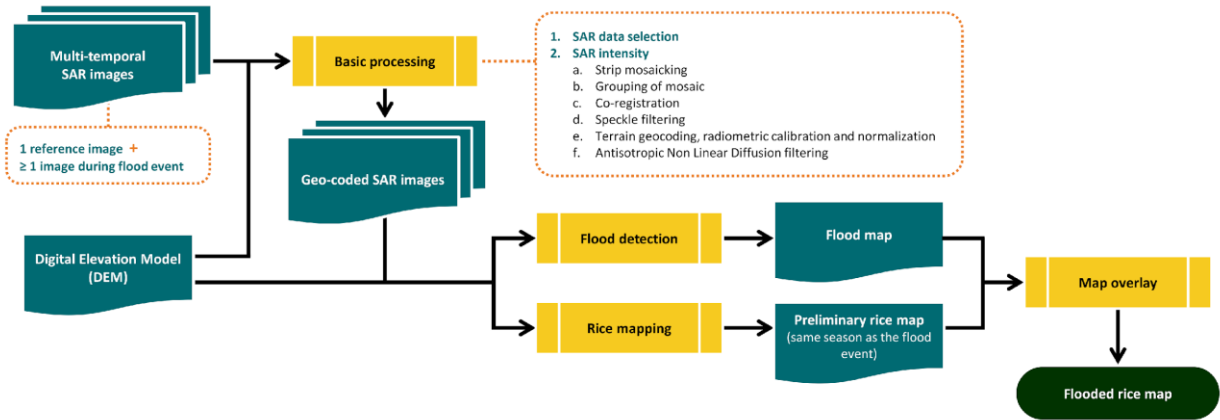


Figure 1. The flood mapping process.

The resulting flood map had the following classes:

1. Not of interest: areas where all input SAR images were above the water threshold.
2. Permanent water: areas where all input SAR images were below the water threshold.
3. Flooded: areas that were not detected as flooded in the reference SAR image but were detected as flooded in the SAR image(s) acquired during the flood event.

Delineating flood-prone areas: All the flood maps from 2014 to 2018 were combined to delineate flood-prone areas. Because the assessments conducted over the course of five years included SAR images with different swath widths and resolutions, resampling and extent redefinition were performed to make the images consistent across all the input layers. The flood maps were overlaid to calculate the number of times each pixel was detected as flooded. Lastly, the flood and rice extent maps were overlaid to derive the frequency of flooding in rice areas. The results were aggregated at the regional and provincial levels.

3. RESULTS

3.1 Typhoon and flood events, 2014-18

The flood assessments that were conducted were mainly due to the occurrence of typhoons or tropical depressions although some assessments were conducted for flooding due to the southwest monsoon in Central Luzon, and due to the tail end of the cold front and heavy rains in the southern regions (Table 3).

Table 3. Estimates of rice, total flooded and flooded rice areas in regions covered by SAR data, 2014-18.

Flood event	Regions assessed	Rice area (ha) ^a	Rice area at risk (ha)	Flooded areas (ha)	Flooded rice areas (ha)
2014					
Typhoon Rammasun	V ^b , VIII ^b	n.a. ^b	n.a. ^b	23,289	n.a. ^b
Tropical storm Fung-wong	III	196,594	n.a.	2,541	2,196
Typhoon Hagupit	CALABARZON ^c , VIII	n.a. ^c 18,997	n.a. n.a.	5,116 1,437	n.a. ^c 591
2015					
Typhoon Mujigae	III	289,044	n.a.	13,559	5,681
Typhoon Koppu	CAR, I, II, III, CALABARZON	614,886	n.a.	62,488	22,205
Typhoon Melor	MIMAROPA,	29,005	29,005	25,672	3,539
2016					
Southwest monsoon	III	314,259	n.a.	38,880 ^d 27,724 ^e	13,666 ^d 10,983 ^e
Typhoon Sarika	V, III	494,530	358,894	59,160	33,234

Table 3. Estimates of rice, total flooded and flooded rice areas in regions covered by SAR data, 2014-18 (cont'd).

Flood event	Regions assessed	Rice area (ha) ^a	Rice area at risk (ha)	Flooded areas (ha)	Flooded rice areas (ha)
Typhoon Haima	CAR, I, II, III, CALABARZON	1,076,548	951,026	96,930	55,116
Severe tropical storm Tokage	MIMAROPA	148,453	17,018	24,814	1,082
Typhoon Nock-ten	CALABARZON, MIMAROPA, V, VI, VII, VIII	593,140	n.a.	45,185	5,219
2017					
Tropical depression 01W (Auring)	VI, VII, VIII, IX, X, XI, XII, XIII, ARMM	263,158	262,360	35,770	8,441
The tail end of a cold front	IX, X, XI, XII, XIII, ARMM	331,898	n.a.	46,527	9,967
Heavy rains	ARMM	3,002	n.a.	7,332	162
Severe tropical storm Pakhar	CAR, I, II, III	438,028	438,028	37,914	17,620
Typhoon Doksuri	I, III, CALABARZON, V	330,812	325,728	12,068	1,052
Tropical storm Kai-tak ^f	V, VI, VII, III	n.a.	n.a.	46,320	n.a.
Typhoon Tembin ^f	VI, VII, VIII, IX, X, XI, XII, XIII, ARMM	n.a.	n.a.	67,973	n.a.
2018					
Tropical storm Son-Tinh and Severe tropical Storm Ampil	I, III, CALABARZON, MIMAROPA, XI	238,482	238,453	17,574	3,102
Tropical depression 13W (Josie), Son-Tinh and Ampil	XII	96,976	95,989	11,284	1,816
Tropical storm Yagi	I, III	182,094	174,737	3,366	505
Tropical depression 24W	CAR, I	270,726	270,715	23,805	10,494
Typhoon Mangkhut	CAR, I, II, III, CALABARZON, MIMAROPA	1,030,955	1,021,261	82,385	31,703
Typhoon Yutu	CAR, I, II, III, CALABARZON, MIMAROPA	1,114,058	240,833	38,148	13,815
Tropical depression 35W (Usman)	V, VI, VII, VIII	59,396	59,396	43,634	2,737

^aRice area estimate in regions assessed at the time of each extreme weather event. ^bThe typhoon happened early in the wet season and many of the rice areas were not yet planted as a result of the dry spell. ^cNo rice area and flooded rice area estimates because the region was not yet part of PRISM in 2014. ^d14 August assessment. ^e21 August assessment. ^fNo rice area and flooded rice area estimates due to expired software license.

Most of the typhoon/flood events occurred during the wet season which coincides with the monsoon (Figure 2). The most frequent and most damaging in terms of rice area flooded were in September and October which coincide with the ripening and peak of harvesting of wet season rice.

3.2 Flooded area

Estimates of flooded area include only those areas still flooded at the date and time of the SAR acquisition. Areas where flood waters had subsided prior were not accounted for in the analysis and therefore flooded areas may be underestimated. An example of detailed estimates of flooded rice area by crop growth phase from the most damaging flood event over the five-year period, Typhoon Haima in 2016, is presented in Table 4.

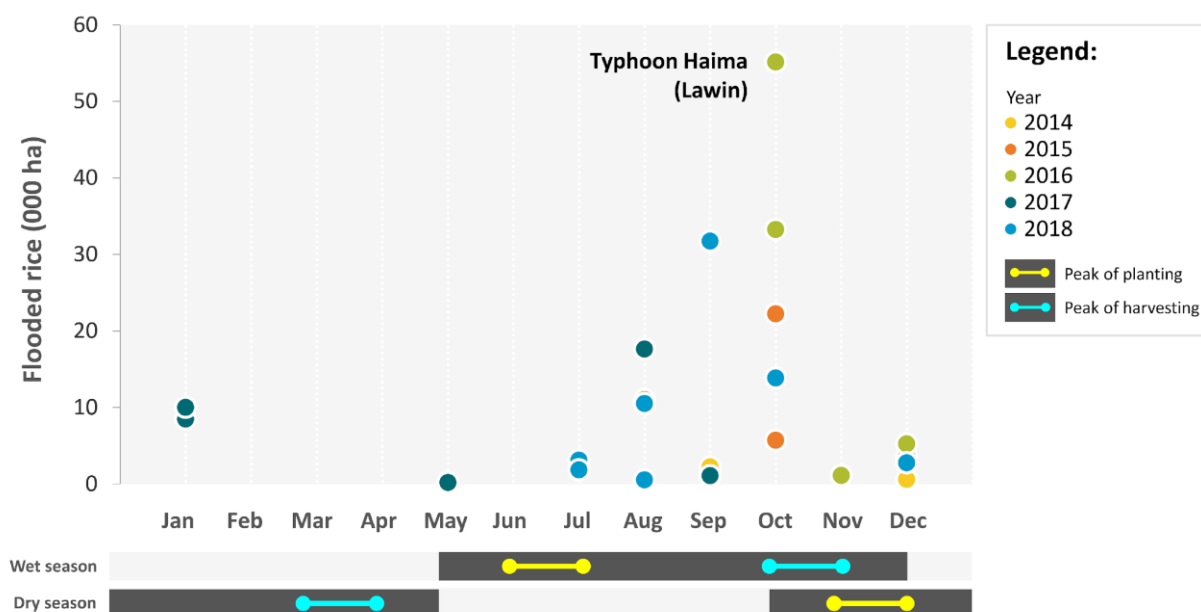


Figure 2. Flooded rice area by month and year of assessment, 2014-18.

Table 4. Estimates of flooded rice area (ha) by crop growth phase on October 20, 2016.

Region/Province	Flooded rice area by crop growth phase (ha)			Flooded with standing rice crop (ha)	Possibly harvested (ha)
	Vegetative	Reproductive	Ripening		
CAR	759	561	96	1,416	15
Abra	173	147	24	344	1
Apayao	407	231	21	659	7
Benguet	0	0	0	0	0
Ifugao	48	86	37	171	0
Kalinga	130	96	14	240	6
Mountain Province	1	2	0	2	0
I-Ilocos Region	3,212	1,095	236	4,544	46
Ilocos Norte	57	26	8	90	0
Ilocos Sur	98	73	8	180	0
La Union	174	112	9	294	0
Pangasinan	2,883	885	211	3,979	45
II-Cagayan Valley	9,525	10,517	2,945	22,987	887
Cagayan	7,106	7,705	2,470	17,281	565
Isabela	1,963	2,209	414	4,587	310
Nueva Vizcaya	439	583	54	1,077	10
Quirino	17	19	6	42	2
III-Central Luzon	11,626	5,265	5,422	22,313	2,478
Aurora	13	20	14	47	8
Bataan	323	87	46	456	21
Bulacan	627	222	462	1,311	112
Nueva Ecija	1,663	784	799	3,247	462
Pampanga	5,341	3,355	3,488	12,184	1,637
Tarlac	3,560	787	597	4,944	228
Zambales	99	10	15	124	10
CALABARZON	217	152	53	422	9
Batangas	54	54	21	130	0
Cavite	54	30	12	96	3
Laguna	18	14	3	35	0
Quezon	82	50	11	143	0
Rizal	9	3	5	18	6
ALL	25,340	17,591	8,751	51,682	3,433

3.3 Flood-prone area

The region with the most number of flood assessments during 2014-2018 was Central Luzon (14), followed by CALABARZON (11). Results from the flood assessments show that 0.3 million ha of rice were flooded at least twice in five years (Table 5) and 16 thousand ha were flooded 4-5 times in five years. Central Luzon, the top rice-producing region in the country, is by far the most flood-prone region with 116 thousand ha of its rice land flooded in at least two out of five years (Figure 3).

Table 5. Total and rice area flooded by region based on flood assessments conducted in 2014 to 2018.

Region	Total flooded area (ha) by frequency (out of 5 years)				Total flooded rice area (ha) by frequency (out of 5 years)			
	At least once	At least 2x	At least 3x	4-5 times	At least once	At least 2x	At least 3x	4-5 times
CAR	19,163	4,564	636	19	14,611	3,337	477	13
I-Ilocos	88,123	24,118	6,325	844	74,296	21,778	5,885	793
II-Cagayan Valley	125,086	28,309	5,289	238	113,080	25,166	4,720	213
III-Central Luzon	299,084	124,294	45,535	13,661	258,732	116,011	43,499	13,352
Calabarzon	26,825	6,241	1,128	104	20,200	5,180	927	88
MIMAROPA	57,896	17,815	2,917	140	52,136	16,915	2,850	139
V-Bicol	76,750	32,897	9,550	724	69,351	32,021	9,459	719
VI-Western Visayas	37,332	6,760	524	4	22,408	4,261	296	2
VII-Central Visayas	10,016	1,509	193	14	5,879	908	121	10
VIII-Eastern Visayas	43,306	8,594	1,246	118	38,642	8,291	1,223	117
IX-Zamboanga Peninsula	28,277	8,128	2,115	198	20,869	7,370	2,050	195
X-Northern Mindanao	18,669	3,981	709	27	14,036	3,688	678	26
XI-Davao Region	19,796	3,192	41	0	17,261	3,026	36	0
XII-SOCCSKSARGEN	39,820	3,979	185	2	30,829	3,320	136	1
XIII-Caraga	47,102	3,146	0	0	36,679	2,911	0	0
ARMM	26,551	2,154	174	3	11,291	708	24	1
TOTAL	963,795	279,679	76,569	16,098	800,299	254,890	72,382	15,669

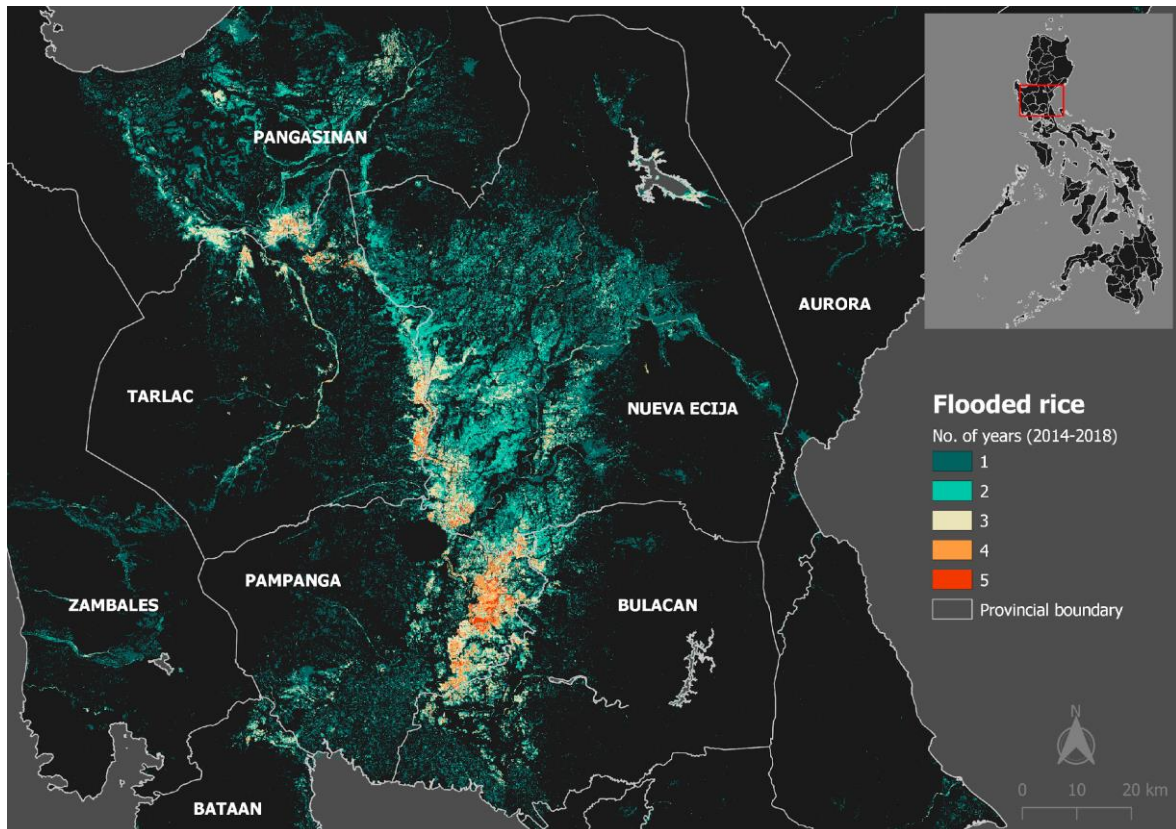


Figure 3. Frequency of flooding in rice fields in parts of Central Luzon, Philippines, 2014-18.

4. CONCLUSION

To provide timely and accurate data on rice area, including damage due to typhoon and flood, PRISM developed and implemented a flood assessment protocol using satellite imagery. Results for flood assessments conducted from 2014 to 2018 were presented. In addition, flood-prone rice and other areas were delineated based on flood assessments conducted over the five-year period.

Results from the flood assessments show that nearly 0.3 million ha of rice were flooded at least twice in five years. Central Luzon, the top rice-producing region in the country, had the most flood-prone rice areas. To mitigate losses, measures such as the promotion of submergence-tolerant rice varieties in these flood-prone rice areas are recommended.

Although SAR has advantages compared with optical systems, particularly for operational flood mapping, some challenges remain (Clement et al., 2017). In particular, shadows in mountainous areas can result in anomalous dark areas within the radar image, which can be misclassified as water (flood). This has been (partially) addressed in this study by masking out these areas using a slope threshold. In addition, heavy rainfall and/or wind can result in roughening of the water surface and hence backscattering of the radar signal, which increases the possibility of inundated areas not being mapped correctly (Alsdorf et al., 2007, Jung et al., 2010). Accurate flood detection depends on the date of the image acquisition. Images acquired too late or when flood waters have already receded will cause underestimation of flooded areas. With the availability of Sentinel-1B images after its launch in 2016, the frequency of SAR image acquisition increased with the reduction in the repeat cycle of up to six days in some areas. The current protocol for assessments of affected area due to typhoons described here refers to flooded areas only. Strong winds during typhoons can cause lodging and bring damage to rice crops. Hence, the estimates provided may be lower than the actual affected areas. Methods for detecting lodging have been tested and applied for wheat (e.g., Yang et al 2015) and maize (e.g., Han et al 2017). These should be tested on rice using data collected at monitoring sites and in field observations during rapid field appraisals and adapted, if needed.

Despite the limitations presented, the flood assessment protocol of PRISM has been used to provide estimates much faster than the current method employed by the DA which is through the mobilization of RFOs and local government units (LGUs).

The timeliness and objectivity of the estimation process and data submission are crucial for decision makers in relation to emergency response and rehabilitation. As part of the operational phase of PRISM, the protocol will continue to be used and improved to increase accuracy.

ACKNOWLEDGMENT

The work presented here was funded by the Philippine Rice Information System (PRISM), a collaborative project involving the Department of Agriculture (DA), Philippine Rice Research Institute (PhilRice), International Rice Research Institute (IRRI), DA-Regional Field Offices (RFOs) and sarmap and is funded by the DA through the DA-Bureau of Agricultural Research.

Sentinel-1SAR data were provided by the Copernicus Sentinel Data (2018) from the European Space Agency.

REFERENCES

- Alsdorf, D.E., Rodriguez, E., Lettenmaier, D.P. 2007. Measuring surface water from space. *Reviews of Geophysics*, 45(2), RG2002. <https://doi.org/10.1029/2006RG000197>.
- Blanc, E., Strobl, E. 2016. Assessing the impact of typhoons on rice production in the Philippines. *Journal of Applied Meteorology and Climatology*, 55(4), pp. 993–1007.
- Cian, F., Marconcini, M., Ceccato, P. 2018. Normalized Difference Flood Index for rapid flood mapping: taking advantage of EO big data. *Remote Sensing*, 209, pp. 712–739.
- Clement, M.A., Kilsby, C.G., Moore, P. 2017. Multi-temporal synthetic aperture radar flood mapping using change detection. *Journal of Flood Risk Management*, 11(2), pp. 152–168.
- Han, D., Yang, H., Yang, G., Qiu, C. 2017. Monitoring model of corn lodging based on Sentinel-1 radar image. SAR in Big Data Era: Models, Methods and Applications (BIGSAR DATA), Beijing, 2017, p 1-5. doi: 10.1109/BIGSAR DATA.2017.8124928.
- IPCC (Intergovernmental Panel on Climate Change). 2014. *Climate Change 2014: Synthesis Report. Contribution of Working Groups I, II, and III to the Fifth Assessment Report of the Intergovernmental Panel on Climate Change* [Core Writing Team, Pachauri RK, Meyer LA (eds.)]. IPCC, Geneva, Switzerland, 151 p.
- IRRI and PhilRice. 2018. *Philippine Rice Information System: Operations Manual, Volume 2*. International Rice Research Institute, Los Baños, Philippines and Philippine Rice Research Institute, Science City of Muñoz, Philippines, 151 p.
- Jung, H.C., Hamski, J., Durand, M., Alsdorf, D., Hossain, F., Lee, H., Hossain, A., Hasan, K., Khan, A.S., Hoque, A. 2010. Characterization of complex fluvial systems using remote sensing of spatial and temporal water level variations in the Amazon, Congo, and Brahmaputra Rivers. *Earth Surface Processes and Landforms*, 35(3), pp. 294–304. <https://doi.org/10.1002/esp.1914>.
- Masutomi, Y., Iizumi, T., Takahashi, K., Yokozawa, M. 2012. Estimation of the damage area due to tropical cyclones using fragility curves for paddy rice in Japan. *Environmental Research Letters*, 7:014020. doi: <https://doi.org/10.1088/1748-9326/7/1/014020>.
- Nelson, A., Setiyono, T., Rala, A.B., Quicho, E.D., Raviz, J.V., Abonete, P.J., et al., 2014. Towards an Operational SAR-Based Rice Monitoring System in Asia: Examples from 13 Demonstration Sites across Asia in the RIICE Project. *Remote Sensing*, 6 (11), 10773-10812.
- PAGASA, 2019. Retrieved September 1, 2019 from <http://bagong.pagasa.dost.gov.ph/>.
- Yang, H., Chen, E., Lia, Z., Zhao, C., Yang, G., Pignatti, S., Casad, R., Zhao, L., 2015. Wheat lodging monitoring using polarimetric index from RADARSAT-2 data. *International Journal of Applied Earth Observation and Geoinformation*, 34, pp. 157–166.